PHYSICAL REVIEW B **85**, 180502(R) (2012)

Mechanism for a pairing state with time-reversal symmetry breaking in iron-based superconductors

Christian Platt,[1] Ronny Thomale,[1,2,3] Carsten Honerkamp,[4] Shou-Cheng Zhang,[3] and Werner Hanke[1]

[1]*Theoretical Physics, University of Würzburg, D-97074 Würzburg*

[2]*Department of Physics, Princeton University, Princeton, New Jersey 08544, USA*

[3]*Department of Physics, McCullough Building, Stanford University, Stanford, California 94305-4045, USA*

[4]*Institute for Theoretical Solid State Physics, RWTH Aachen University and JARA–FIT Fundamentals of Future Information Technology, D-52056 Aachen*

(Received 27 July 2011; revised manuscript received 31 January 2012; published 10 May 2012)

The multipocket Fermi surfaces of iron-based superconductors promote pairing states with both extended s-wave and d-wave symmetry. We argue that the competition between these two order parameters could lead to a time-reversal symmetry-breaking state with $s + id$ pairing symmetry in the iron-based superconductors, and propose several scenarios in which this phase may be found. To understand the emergence of such a pairing state on a more rigorous footing, we start from a microscopic five-orbital description representative of the pnictides. Using a combined approach of functional renormalization-group and mean-field analysis, we identify the microscopic parameters of the $s + id$ pairing state. There, we find the most promising region for $s + id$ pairing in the electron-doped regime with an enhanced pnictogen height.

DOI: 10.1103/PhysRevB.85.180502 PACS number(s): 74.20.Mn, 71.10.Fd, 74.20.Rp

Iron-based superconductors (SC) offer an appealing platform to investigate the interplay among pairing interactions, pairing symmetries, and Fermi-surface topologies.[1] Generally, repulsive interactions in momentum space can lead to a change of sign in the pairing amplitude. A large class of iron-based SC have disconnected Fermi-surface pockets, consisting of hole pockets at the $\Gamma = (0,0)$ and possibly $M = (\pi,\pi)$ points, and two electron pockets at the $X = (\pi,0)/(0,\pi)$ points in the unfolded Brillouin zone (BZ) with one iron atom per unit cell. When the repulsive interactions between the hole and the electron pockets dominate, an $s_\pm$ pairing symmetry can be obtained.[2–4] On the other hand, when the repulsive interactions between the two electron pockets dominate, a propensity toward d-wave pairing symmetry can be expected, where the form factor follows the extended d-wave gap function to optimize electron-hole scattering as introduced by us in Ref. 5. When both types of interactions are comparable, there is hence a frustration between the two types of pairing symmetry. A recent theoretical proposal suggests that the system can resolve the frustration by a pairing state with $s + id$ pairing symmetry which spontaneously breaks time-reversal (TR) symmetry.[6] The possibility of a TR symmetry-breaking pairing state due to frustrating pairing interactions among three or more Fermi pockets has also been investigated in several other contexts.[7–13] In general, time-reversal breaking pairing states have rather accessible experimental signatures, and several proposals have been suggested in the context of iron-based SC.[6]

In principle there are various experimentally tunable parameters to drive the competition between the s wave and d wave in the pnictides, giving the opportunity to start from both limits. In $K_xBa_{1-x}Fe_2As_2$, the Fermi-surface topology can be chosen as a paradigmatic setup for $s_\pm$, consisting of hole pockets at Γ and the electron pockets at X for optimal doping $x \simeq 0.4$. Upon increasing x, however, the electron pockets decrease, and have nearly disappeared for $x = 1$ (Fig. 1), which has been recently suggested to host a d-wave pairing symmetry.[14] In this system, it is hence plausible that an $s + id$ pairing state can be realized for intermediate values of x. In the chalcogenide $K_xFe_{2-y}Se_2$, the electron pockets at the X points dominate, and, for a situation seemingly inverse to KFe_2As_2, a d-wave pairing symmetry may likewise be expected.[15,16] (It should be noted that the actual pairing symmetry in the chalcogenides is far from settled, as a strong coupling perspective may likewise suggest $s_\pm$ pairing.[17]) By tuning doping or other possible parameters affecting the band structure, such as pressure, one possibly induces a pocket at Γ, increasing the tendency toward $s_\pm$ pairing symmetry (Fig. 1). In this case, one could also expect an $s + id$ pairing state. By systematically tuning the Fermi pocket topologies, one can compare the predicted pairing symmetries with experiments, and determine the nature of the pairing interaction by these investigations, starting from compound settings with a suspected d-wave symmetry (Fig. 1).

In the following, we rather intend to start from an $s_\pm$ pairing state instead, and address how we can enhance the competitiveness of the d-wave symmetry to drive the system into the $s + id$ regime. The reason for this is twofold. First, the $s_\pm$ symmetry is much more generic for the different classes of pnictides. Second, as we will see below, we find the most promising setup to be located on the electron-doped side of pnictides, where high-quality samples have already been grown for different families. We hence believe that this regime may be the experimentally most accessible scenario at the present stage, which is why we explicate it in detail. In this paper, we investigate the microscopic mechanism of the $s + id$ pairing state by the functional renormalization-group (fRG) method of a five-band model. We systematically vary the doping level and the strength of intraorbital interaction, which determine the ratio between the electron-hole pocket and the electron-electron pocket mediated pairing interactions. In this microscopic investigation, we find that the $s + id$ pairing state can be realized in the intermediate electron-doped regime, given that we also adjust the pnictogen height parameter of the system appropriately.

We start from a representative five-band model for the pnictides which is obtained from local-density approximation (LDA) -type calculations.[3] It has been considered by us before

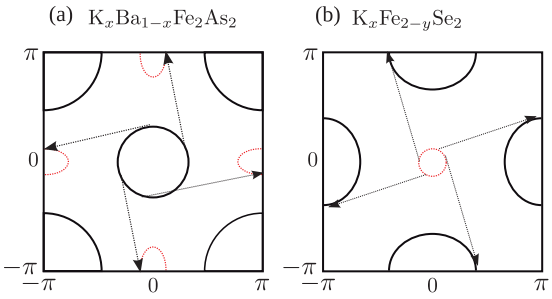

FIG. 1. (Color online) Frustrating the d-wave limits of KFe_2As_2 (a) and $K_xFe_{2-y}Se_2$ (b). Upon doping or differently induced band-structure effects, electron pockets appear (dashed red) in (a) and a hole pocket appears (dashed red) in (b) which populate the $q \sim (\pi,0)/(0,\pi)$ scattering channels enhancing the $s_\pm$ symmetry. This leads to frustration providing the background for $s + id$ pairing.

as a starting point for explaining the difference between the isovalent P-based and As-based pnictides.[18] The LDA "noninteracting" part is given by

$$H_0 = \sum_{\boldsymbol{k},s} \sum_{a,b=1}^{5} c^\dagger_{\boldsymbol{k}as} K_{ab}(\boldsymbol{k}) c_{\boldsymbol{k}bs}. \tag{1}$$

Here, c's stand for electron annihilation operators, a and b stand for the d orbitals, s denotes the spin indices, and $K_{ab}(\boldsymbol{k})$ stands for the orbital (i.e., maximally localized Wannier function) matrix elements of the Kohn-Sham Hamiltonian. The band structure features electron pockets at X and hole pockets at Γ, which is the typical situation in the pnictides (Fig. 2) for sufficient electron doping. The many-body interaction part is given by the intra- and interorbital interactions U_1 and U_2, as well as the Hund's coupling $J_{\rm H}$ and the pair hopping $J_{\rm pair}$:

$$H_{\rm int} = \sum_i \Bigg[U_1 \sum_a n_{i,a\uparrow} n_{i,a\downarrow} + U_2 \sum_{a<b,s,s'} n_{i,as} n_{i,bs'} + \sum_{a<b} \Bigg(J_{\rm H} \sum_{s,s'} c^\dagger_{ias} c^\dagger_{ibs'} c_{ias'} c_{ibs} + J_{\rm pair} c^\dagger_{ia\uparrow} c^\dagger_{ia\downarrow} c_{ib\downarrow} c_{ib\uparrow} \Bigg) \Bigg], \tag{2}$$

where $n_{i,as}$ denote density operators at site i of spin s in orbital a. Typical interaction settings are dominated by intraorbital coupling, $U_1 > U_2 > J_{\rm H} \sim J_{\rm pair}$. In the fRG,[5,18–22] one starts from the bare many-body interaction (2) in the Hamiltonian. The pairing is dynamically generated by systematically integrating out the high-energy degrees of freedom including the important fluctuations (magnetic, SC, screening, vertex corrections) on equal footing. This differs from the random-phase approximation, which takes right from the outset a magnetically driven spin-fluctuation type of pairing interaction. For a given instability characterized by some order parameter $\hat{O}_{\boldsymbol{k}}$, the effective interaction vertex $V_\Lambda(\boldsymbol{k}_1,\boldsymbol{k}_2,\boldsymbol{k}_3,\boldsymbol{k}_4)$ in a particular ordering channel can be written in shorthand notation as $\sum_{\boldsymbol{k},\boldsymbol{p}} V_\Lambda(\boldsymbol{k},\boldsymbol{p})[\hat{O}^\dagger_{\boldsymbol{k}} \hat{O}_{\boldsymbol{p}}]$. Accordingly, the effective interaction vertex $V_\Lambda(\boldsymbol{k},-k,\boldsymbol{p},-p)$ in the Cooper channel can be decomposed into different eigenmode contributions[18,19]

$$V^{\rm SC}_\Lambda(\boldsymbol{k},\boldsymbol{p}) = \sum_i c^{\rm SC}_i(\Lambda) f^{{\rm SC},i}(\mathbf{k})^* f^{{\rm SC},i}(\boldsymbol{p}), \tag{3}$$

where i is a symmetry decomposition index, and the leading instability of that channel corresponds to an eigenvalue $c^{\rm SC}_1(\Lambda)$ first diverging under the flow of Λ. $f^{{\rm SC},i}(\boldsymbol{k})$ is the SC form factor of pairing mode i, which tells us about the SC pairing symmetry and hence the gap structure associated with it. In the fRG, from the final Cooper channel in the effective interaction vertex, this quantity is computed along the discretized Fermi surfaces [Fig. 2(a3)], and the leading SC instabilities are plotted in Figs. 2(a1) and 2(b1). The interaction parameters are kept fixed at the representative setup $U_1 = 2.5$ eV, $U_2 = 2.2$ eV, $J_{\rm H} = 1.2$ eV, $J_{\rm pair} = 0.2$ eV (U_1 for the $d_{X^2-Y^2}$ orbital is varied as explicitly stated in Figs. 2 and 3). The relatively large bare value of J_H is motivated partly by recent findings, in particular, for a sizable Hund's rule coupling.[23,24] Furthermore, as a parameter trend, larger $J_{\rm H}$ and smaller $J_{\rm pair}$ tends to prefer the $s + id$ phase in the electron-doped regime for rather moderate values of intraorbital coupling U_1 (Fig. 3).

The situation in Fig. 2 is representative for moderate electron doping and interaction scales of the pnictides, where the $\Gamma \leftrightarrow X$ pair scattering between the hole pockets at Γ and the electron pockets at X dominates. Already from the BCS gap equation, a finite momentum transfer can induce pairing only when the wave vector of such an interaction connects regions on one Fermi surface (FS) (such as in the cuprate case), or regions on different FSs (such as in the pnictide case), which have opposite signs of the SC order parameter. This corresponds to putting the electron pairs in an anisotropic wave function such as sign-reversing s wave ($s_\pm$) in Fig. 2(a), where the wave vector $(\pi,0)$ in the unfolded BZ connects hole and electron pockets with a sign-changing $s_\pm$ gap.[2,4] However, in the fRG calculation of Fig. 2(b) with increased U_1 interaction on the $d_{X^2-Y^2}$ orbital, a green arrow for $X \leftrightarrow X$ scattering indicates additional interactions that become similarly as important as the $(\pi,0)$ channel. This increased U_1 can be tuned by the pnictogen height as explained below and frustrates the previous "pure" $s_\pm$ limit ($\Gamma \leftrightarrow X$). The system then strikes a compromise[18,25] by enhancing the anisotropy of the $s_\pm$ form factor [denoted by $f^{\rm SC}(\boldsymbol{k})$ in Fig. 2] on the electron pockets at X. Throughout this variation of parameters, the sign-changing d-wave form factor (not shown) remains nearly unchanged, providing nodes on the hole pockets and gaps on the electron pockets as they do not intersect with the nodal d-wave lines $k_x = \pm k_y$ in the Brillouin zone. This is because the d-wave-driving $X \leftrightarrow X$ scattering is hardly affected by this change of parameters. Instead, the $s_\pm$ form factor changes significantly, and adjusts the momentum dependence of the gap, i.e., its anisotropy, so as to minimize the effect of the Coulomb repulsion (Fig. 2).

We now have all the ingredients to tune the pairing symmetry from $s_\pm$ wave to extended $d_{x^2-y^2}$ wave, and, eventually, into the TR symmetry-broken $s + id$ phase. In most of the iron-based SC, the tendency toward $s_\pm$ pairing occurs slightly more pronounced than the competing extended $d_{x^2-y^2}$ pairing, and, at first glance, the resulting frustration appears to be too small for causing $s + id$ pairing. Therefore, in order to increase frustration, we somehow have to enhance the pair scattering between the electron pockets at X, which then promotes the subleading $d_{x^2-y^2}$ channel. As shown in *a priori* determinations of the interaction in Eq. (2), expressed in terms of orbital matrix elements, the pnictogen height h_p

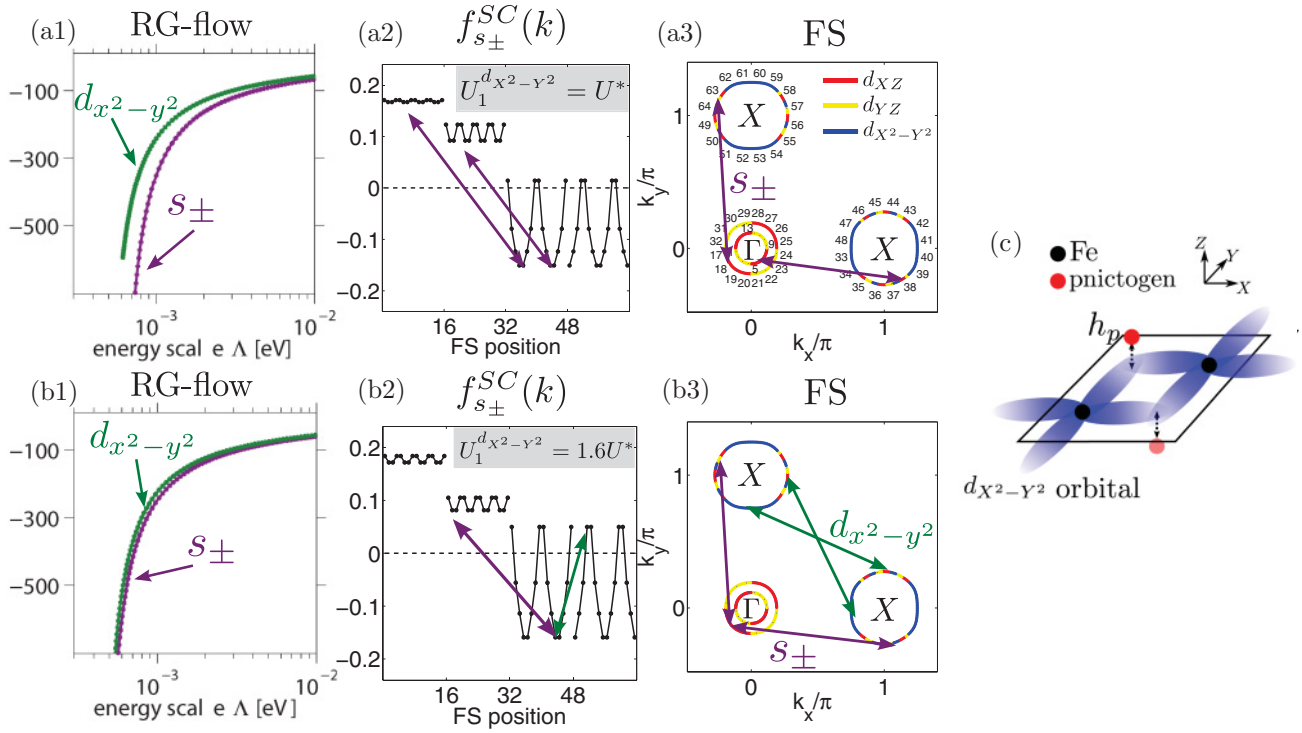

FIG. 2. (Color online) Competing pairing orders and s-wave SC form factors for $U_1(d_{X^2-Y^2}) = U_1^* = 2.5$ eV (a) and $U_1(d_{X^2-Y^2}) = 1.6U^*$ (b) at electron-doped filling $n = 6.13$. RG channel flow [(a1),(b1)] and $s_\pm$-gap form factor [(a2),(b2)]. s/d transition from (a) to (b): Increasing $U_1(d_{X^2-Y^2})$ enhances the gap anisotropy of the $s_\pm$ form factor on the electron pockets [$\boldsymbol{k}$ patching: points 33–64; see (a3)] shown in (a2) and (b2) until extended $d_{x^2-y^2}$ becomes competitive. The d-wave form factor (not shown) does not change from (a) to (b). [(a3),(b3)] Interactions mediated by U_1, inducing $s_\pm$-pairing tendency ($\Gamma \leftrightarrow X$) and competing $d_{x^2-y^2}$-pairing symmetry due to ($X \leftrightarrow X$). (c) Variation of the pnictogen height h_p mostly affects the spread of the $d_{X^2-Y^2}$ orbital and thus $U_1(d_{X^2-Y^2})$, as it is oriented to the planar projection of the pnictogen.

[measured from the Fe-plane; Fig. 2(c)] has a substantial influence on the intraorbital interaction U_1 between $d_{X^2-Y^2}$ Wannier orbitals,[26] which can be either modified by isovalent doping or pressure. By increasing h_p, the Wannier functions in this orbital are further localized, causing an increase of $U_1(d_{X^2-Y^2})$. In Fig. 2(b), we have already used this fact to demonstrate that, for moderate e doping (13%), large values of this matrix element drive the SC instability from $s_\pm-$ to extended $d_{x^2-y^2}$-wave symmetry. Note that in the situation where we expect $s + id$ to occur, both the d wave and s wave exhibit nodal features in the form factor.

For this general scenario, we present our predictions for TR symmetry breaking in a schematic phase diagram in Fig. 3, where we plot the leading $s_\pm$, $d_{x^2-y^2}$, and finally $s + id$ SC solutions as a function of $U_1(d_{X^2-Y^2})$, and electron doping. There, we have used our fRG result as a starting point for a renormalized mean-field (MF) analysis.[27] In this MF + fRG approach, the one-loop flow is stopped at a scale Λ, which is small compared to the bandwidth, but still safely above the scale Λ_c, where the two-particle vertex diverges. In this range, the particular choice of the cutoff Λ does not significantly influence the results in Fig. 3. The renormalized coupling function $V^\Lambda(\boldsymbol{k}_1,\boldsymbol{k}_2,\boldsymbol{k}_3,\boldsymbol{k}_4)$ is taken as an input for the mean-field treatment of the remaining modes. As shown in Fig. 2, the regime of $s_\pm/d$-wave pairing competition features a single-channel SC instability without other competing (e.g., magnetic) instabilities and, therefore, justifies

$$V^\Lambda(\boldsymbol{k}_1,\boldsymbol{k}_2,\boldsymbol{k}_3,\boldsymbol{k}_4) \approx V^{\text{pair}}(\boldsymbol{k}_1,\boldsymbol{k}_3)\delta_{\boldsymbol{k}_2,-\boldsymbol{k}_1}\delta_{\boldsymbol{k}_4,-\boldsymbol{k}_3}, \qquad (4)$$

with $V^{\text{pair}}(\boldsymbol{k}_1,\boldsymbol{k}_3) = V^\Lambda(\boldsymbol{k}_1,-\boldsymbol{k}_1,\boldsymbol{k}_3,-\boldsymbol{k}_3)$. The effective theory for quasiparticles near the Fermi surface ($|\xi(\boldsymbol{k})| < \Lambda$)

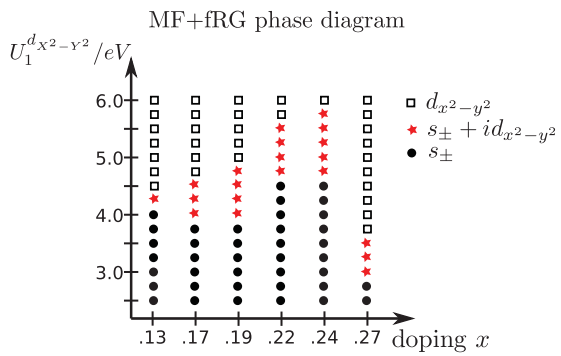

FIG. 3. (Color online) Preferred pairing as a function of electron doping and intraorbital Coulomb interaction $U_1(d_{X^2-Y^2})$. The results are obtained by minimizing the mean-field free energy of the effective theory taken from fRG at $\Lambda \approx 0.001$ eV. At 27% electron doping, the $s + id$ pairing state occurs at $U_1(d_{X^2-Y^2}) = 3$ eV, which is comparable to the intraorbital repulsion in the remaining orbitals $U_1 = 2.5$ eV.

is modeled by the reduced Hamiltonian

$$H^{\Lambda} = \sum_{ks} \xi(\boldsymbol{k}) c^{\dagger}_{ks} c_{ks} + \frac{1}{N} \sum_{k,q} V^{\text{pair}}(\boldsymbol{k},\boldsymbol{q}) c^{\dagger}_{k\uparrow} c^{\dagger}_{-k\downarrow} c_{-q\downarrow} c_{q\uparrow}, \tag{5}$$

where $\xi(\boldsymbol{k})$ is taken as the bare dispersion due to only weak band-renormalization effects. The MF solution of this reduced Hamiltonian is obtained as in BCS theory, by solving the self-consistent gap equation and calculating the corresponding grand potential, which is

$$\Omega^{\text{stat}} = -\sum_{k} \frac{|\Delta_k|^2 + 2\xi(\boldsymbol{k})^2}{2\sqrt{\xi(\boldsymbol{k})^2 + |\Delta_k|^2}} + \sum_{k} \xi(\boldsymbol{k}). \tag{6}$$

Within a reasonable range of parameters for the electron-doped pnictides, we then find a regime favoring $s + id$ pairing due to

$$\Omega^{\text{stat}}_{s+id} < \Omega^{\text{stat}}_{s_{\pm}}, \Omega^{\text{stat}}_{d}. \tag{7}$$

The system hence prefers to evolve into a TR-broken superconducting state. This is intuitive from the viewpoint of condensation energy in the SC phase. While both s and d waves possess nodal features individually, the combination $s + id$ allows one to avoid the nodes which are stabilizing the condensate.

Note that the phase regime investigated by us is only a lower bound for the possible existence of $s + id$, which may even be larger. This is because the fRG setup at present only allows us to obtain the leading SC instability at some finite Λ_c, while the $s + id$ phase may well set in below Λ_c. This would manifest itself as a change of the SC phase as a function of temperature in experiment.

In summary, we have presented a microscopic analysis, based on *a priori* electronic structure determinations and a combination of the fRG with an MF treatment of the remaining low-energy states, to derive a kind of "guiding principle" for a possible $s + id$ pairing state in the pnictides. For the case of increased electron doping and pnictogen height, we have illustrated how this drives the system into an $s + id$ SC state. Aside from this example, other regimes in the pnictides likewise promise the possible realization of an $s + id$ state, such as hole-doped (K,Ba)-122 interpolating between the s-wave limit ($x \sim 0.4$) and d-wave limit ($x \sim 1$) as well as possibly the chalcogenides $K_xFe_{2-y}Se_2$.

We thank A. V. Chubukov, D. Scalapino, and P. Hirschfeld for discussions. S.C.Z. is supported by NSF DMR-0904264, C.P., R.T., C.H., and W.H. are supported by DFG-SPP 1458/1, C.P., C.H., and W.H. are supported by DFG-FOR 538, and R.T. is supported by the Humboldt Foundation.

[1] Y. Kamihara, T. Watanabe, M. Hirano, and H. Hosono, J. Am. Chem. Soc. **130**, 3296 (2008).
[2] I. I. Mazin, D. J. Singh, M. D. Johannes, and M. H. Du, Phys. Rev. Lett. **101**, 057003 (2008).
[3] K. Kuroki, S. Onari, R. Arita, H. Usui, Y. Tanaka, H. Kontani, and H. Aoki, Phys. Rev. Lett. **101**, 087004 (2008).
[4] A. V. Chubukov, D. V. Efremov, and I. Eremin, Phys. Rev. B **78**, 134512 (2008).
[5] R. Thomale, C. Platt, J. Hu, C. Honerkamp, and B. A. Bernevig, Phys. Rev. B **80**, 180505 (2009).
[6] W. C. Lee, S. C. Zhang, and C. Wu, Phys. Rev. Lett. **102**, 217002 (2009).
[7] Y. Ren, J.-H. Xu, and C. S. Ting, Phys. Rev. B **53**, 2249 (1996).
[8] J.-X. Zhu, W. Kim, and C. S. Ting, Phys. Rev. B **57**, 13410 (1998).
[9] D. F. Agterberg, V. Barzykin, and L. P. Gorkov, Phys. Rev. B **60**, 14868 (1999), and references therein.
[10] T. K. Ng and N. Nagaosa, Europhys. Lett. **87**, 17003 (2009).
[11] V. Stanev and Z. Tesanovic, Phys. Rev. B **81**, 134522 (2010).
[12] Y. Tanaka and T. Yanagisawa, J. Phys. Soc. Jpn. **79**, 114706 (2010).
[13] X. Hu and Z. Whang, e-print arXiv:1103.0123v2.
[14] R. Thomale, C. Platt, W. Hanke, J. Hu, and B. A. Bernevig, Phys. Rev. Lett. **107**, 117001 (2011).
[15] T. A. Maier, S. Graser, P. J. Hirschfeld, and D. J. Scalapino, Phys. Rev. B **83**, 100515(R) (2011).
[16] F. Wang, F. Yang, M. Gao, Z.-Y. Lu, T. Xiang, and D.-H. Lee, Europhys. Lett. **93**, 57003 (2011).
[17] C. Fang, Y.-L. Wu, R. Thomale, B. A. Bernevig, and J. Hu, Phys. Rev. X **1**, 011009 (2011).
[18] R. Thomale, Ch. Platt, W. Hanke, and B. A. Bernevig, Phys. Rev. Lett. **106**, 187003 (2011).
[19] F. Wang, H. Zhai, Y. Ran, A. Vishwanath, and D.-H. Lee, Phys. Rev. Lett. **102**, 047005 (2009).
[20] C. Platt, C. Honerkamp, and W. Hanke, New J. Phys. **11**, 055058 (2009).
[21] C. Honerkamp, M. Salmhofer, N. Furukawa, and T. M. Rice, Phys. Rev. B **63**, 035109 (2001).
[22] W. Metzner, M. Salmhofer, C. Honerkamp, V. Meden, and K. Schönhammer, Rev. Mod. Phys. **84**, 299 (2012).
[23] J. Zhang, R. Sknepnek, R. M. Fernandes, and Jörg Schmalian, Phys. Rev. B **79**, 220502(R) (2009).
[24] K. Haule and G. Kotliar, New J. Phys. **11**, 02502 (2009).
[25] C. Platt, R. Thomale, and W. Hanke, Ann. Phys. (Berlin) **523**, 638 (2011).
[26] For a recent review see M. Imada and T. Miyake, J. Phys. Soc. Jpn. **79**, 112001 (2010).
[27] J. Reiss, D. Rohe, and W. Metzner, Phys. Rev. B **75**, 075110 (2007).